Advanced Review

Quantum Monte Carlo methods

Arne Lüchow*

Simulations of complex systems have seen rapid progress over the last decade not only due to the continuous acceleration of computer resources but also due to improvements of methods and algorithms. Simulations complement experiments and model calculations in the effort to get insight into complex systems such as materials, complex liquids, or complicated molecules. As such, computer simulations are a strongly interdisciplinary field where chemistry meets physics, biology, and material science. Most simulations are based on classical physics because the interaction between atoms or even larger entities can be modeled accurately with classical mechanics for most problems as long as no chemical reactions are involved. If the interaction between atoms in a molecule or between molecules is to be calculated, for instance, to obtain parameters for modeling the interactions in classical simulations, classical physics has to be abandoned because these interactions involve the electron distributions which require a quantum mechanical description. © 2011 John Wiley & Sons, Ltd. *WIREs Comput Mol Sci* 2011 1 388–402 DOI: 10.1002/wcms.40

INTRODUCTION

In this advanced review, a Monte Carlo-based quantum simulation technique is described, which is able to calculate accurately the electronic energy of molecules and the interaction energy between molecules. It is a main characteristic of the quantum Monte Carlo (QMC) methods that the electron distribution is obtained from a random walk of the electrons. Similarly, energy and properties of liquids or solids are obtained from random walk trajectories of the atoms or molecules in classical Monte Carlo simulations. One may wonder how electron trajectories in random walks can make any physical sense as electrons are indistinguishable and have to obey the Heisenberg uncertainty principle that prohibits the existence of electron trajectories. In the following section, the method is explained in more detail; here it may suffice to mention that the electrons in QMC follow trajectories in imaginary time where the uncertainty principle does not hold. It is the role of the trajectories to sample the electron distribution, allowing the analysis of the distribution as well as the accurate statistical calculation of the energy.

The most common methods to calculate electronic structure are density functional methods (DFT) or wavefunction-based methods such as Hartree–Fock (HF) or many-body perturbation approaches. These two types of methods differ considerably from the QMC approach. DFT is a one-electron mean-field technique, where the electron–electron correlation and the quantum mechanical electron exchange are accounted for by functionals whose exact form is unknown. Wavefunction-based methods approximate the exact wavefunction by expansions in terms of Slater determinants of molecular orbitals (MO). Although all types of methods benefit from a higher speed of computers, Monte Carlo methods are particularly well suited for parallel computations as individual random walkers may be distributed easily among the computing nodes. The current trend in high-performance computing is toward massively parallel systems, which also become more and more heterogeneous as, for instance, graphics chips are increasingly used as inexpensive parallel computing resource.

The review is organized as follows. In the next section, the quantum Monte Carlo methods are described and, in the following section, recent applications are discussed with emphasis on systems that are challenging for electronic structure methods such as transition metal compounds and weakly interacting molecules.

QUANTUM MONTE CARLO METHODS

The quantum Monte Carlo methods have been presented in several review articles[1–3] and a monograph,[4]

*Correspondence to: luechow@pc.rwth-aachen.de

Institut für Physikalische Chemie, RWTH Aachen University, Aachen, Germany

DOI: 10.1002/wcms.40

and therefore only an overview will be given. The two most important methods are called variational quantum Monte Carlo (VMC) and diffusion quantum Monte Carlo (DMC). The VMC technique is simpler as well as more efficient than the DMC method, but usually also less accurate. It is based on the Monte Carlo integration of the Rayleigh–Ritz quotient, whereas the DMC approach has its origin in the observation that the Schrödinger equation in imaginary time τ (and Hartree atomic units)

$$\frac{\partial \psi}{\partial \tau} = -H\psi, \quad H = -\frac{1}{2}\Delta + V \tag{1}$$

is mathematically a diffusion equation and that its stationary solution is the lowest eigenfunction ψ_0 of the Hamiltonian H. This analogy between the Schrödinger equation and a diffusion process has been first described by Erwin Schrödinger in 1931.[5] J. B. Anderson has recently published a little book describing briefly the most important papers for the development of the quantum Monte Carlo methods starting with Schrödinger's and ending in 2005.[6]

Variational Quantum Monte Carlo Method

In the VMC method, the Rayleigh–Ritz quotient for a trial function ϕ_T is evaluated with Monte Carlo integration

$$E_{\mathrm{VMC}} = \frac{\int \phi_T^*(\mathbf{R}) H \phi_T(\mathbf{R}) \mathrm{d}\mathbf{R}}{\int \phi_T^*(\mathbf{R}) \phi_T(\mathbf{R}) \mathrm{d}\mathbf{R}}. \tag{2}$$

$\mathbf{R}$ is used throughout this review for the collection of the cartesian coordinates of n electrons: $\mathbf{R} \in \mathbb{R}^{3n}$, with $\mathbf{R} = (\mathbf{r}_1, \mathbf{r}_2, \ldots, \mathbf{r}_n)$, $\mathbf{r}_i = (x_i, y_i, z_i)$, and Δ to denote the $3n$-dimensional Laplacian. $V = V(\mathbf{R})$ denotes the potential energy, which includes the Coulombic electron nucleus attraction and the electron electron repulsion.

The trial function ϕ_T is usually of the Slater–Jastrow type, which is a product of a Slater determinant, and a Jastrow correlation function that accounts for the correlated movements of the electrons due to their mutual repulsion. The Slater determinant is usually a Hartree–Fock wavefunction or built from Kohn–Sham orbitals of a DFT calculation. The Jastrow correlation function has to be constructed prior to a VMC calculation. Trial functions are discussed in more detail in section *Trial and Guide Functions in Quantum Monte Carlo*. The Metropolis–Hastings algorithm[7,8] is used to sample the distribution

$$p_T(\mathbf{R}) = \frac{\phi_T^*(\mathbf{R}) \phi_T(\mathbf{R})}{\int \phi_T^*(\mathbf{R}) \phi_T(\mathbf{R}) \mathrm{d}\mathbf{R}}, \tag{3}$$

and with a sample $\{\mathbf{R}_i\}_{i=1,\ldots,M}$ of size M of this distribution. With this distribution, the VMC energy can be expressed in terms of the local energy E_{L}:

$$E_{\mathrm{L}}(\mathbf{R}) = \frac{H\phi(\mathbf{R})}{\phi(\mathbf{R})}, \tag{4}$$

the most important quantity in quantum Monte Carlo methods. It should be noted that the local energy is a constant and equal to the eigenvalue E_i if the trial function is an eigenfunction $\psi_i(\mathbf{R})$. The VMC energy is simply the local energy averaged over the distribution $p_T(\mathbf{R})$:

$$E_{\mathrm{VMC}} = \frac{\int \phi_T^*(\mathbf{R}) H \phi_T(\mathbf{R}) \mathrm{d}\mathbf{R}}{\int \phi_T^*(\mathbf{R}) \phi_T(\mathbf{R}) \mathrm{d}\mathbf{R}} = \int E_{\mathrm{L}}(\mathbf{R}) p_T(\mathbf{R}) \mathrm{d}\mathbf{R}$$
$$= \lim_{M\to\infty} \frac{1}{M} \sum_{i=1}^{M} E_{\mathrm{L}}(\mathbf{R}_i). \tag{5}$$

Equation (5) indicates that the VMC energy is calculated with Monte Carlo integration as mean of the local energy. The Metropolis–Hastings method employs a propagation step that is accepted or rejected. The series of propagation steps forms a random walk with a walker being the collection of all electrons $\mathbf{R}$. The Metropolis–Hastings algorithm allows for a fairly arbitrary form of propagator, and it has been found that the drift–diffusion step of the DMC algorithm described below is a very efficient. Although the derivations of DMC and VMC are very different, both methods turn out to share most of the algorithms.

Diffusion Quantum Monte Carlo Method

The solution of the time-dependent Schrödinger equation in imaginary time Eq. (1) for time-independent Hamilton operators H is the lowest eigenfunction ψ_0 of H. This can be easily seen by expanding the solution $\psi(\tau)$ in terms of eigenfunctions ψ_k of H:

$$H\psi_k = E_k \psi_k. \tag{6}$$

Assuming that $\{\psi_k\}$ forms a complete set of square-integrable functions, the solution of Eq. (1), $\psi(\tau)$, can be expressed in terms of the ψ_k subject to the initial condition $\psi(0) = \phi_0$:

$$|\psi(t)\rangle = \sum_k a_k \mathrm{e}^{-E_k \tau} |\psi_k\rangle, \quad a_k = \langle \psi_k | \phi_0 \rangle. \tag{7}$$

This formal solution demonstrates the convergence of $\psi(\tau)$ toward ψ_0. The convergence is exponential and its rate depends on the energy gap $E_1 - E_0$ of the lowest two eigenvalues.

Alternatively, the solution of Eq. (1) can be expressed with the fundamental solution, or Green's

© 2011 John Wiley & Sons, Ltd.

17590884, 2011, 3, Downloaded from https://wires.onlinelibrary.wiley.com/doi/10.1002/wcms.40 by TEI of Greece, Wiley Online Library on [11/12/2025]. See the Terms and Conditions (https://onlinelibrary.wiley.com/terms-and-conditions) on Wiley Online Library for rules of use; OA articles are governed by the applicable Creative Commons License

function, as

$$\psi(\tau, \mathbf{R}) = \int G(\tau, \mathbf{R}', \mathbf{R})\phi_0(\mathbf{R}')\mathrm{d}\mathbf{R}', \tag{8}$$

where $G(\tau, \mathbf{R}, \mathbf{R}')$ is the solution of Eq. (1) with the initial value $G(0, \mathbf{R}, \mathbf{R}') = \delta(|\mathbf{R} - \mathbf{R}'|)$. $G(\tau, \mathbf{R}, \mathbf{R}')$ is the position representation of the propagator $\mathrm{e}^{-\tau H}$ which formally solves Eq. (1):

$$G(\tau, \mathbf{R}, \mathbf{R}') = \langle \mathbf{R}'|\mathrm{e}^{-\tau H}|\mathbf{R}\rangle. \tag{9}$$

$G(\tau, \mathbf{R}, \mathbf{R}')$ describes the propagation from $\mathbf{R}$ to $\mathbf{R}'$ in (imaginary) time τ.

It should be pointed out that the imaginary time operator $\mathrm{e}^{-\tau H}$ is formally identical to the Boltzmann operator $\mathrm{e}^{-\beta H}$ of statistical thermodynamics, where $\beta = 1/kT$. Therefore, ground state DMC simulations, where the long-time limit of $\mathrm{e}^{-\tau H}$ is calculated, and low-temperature simulations with the Boltzmann operator $\mathrm{e}^{-\beta H}$ share considerable agreement in terms of methods and algorithms.

The Green's function satisfies the Chapman–Kolmogorov equation

$$G(\tau_1 + \tau_2, \mathbf{R}, \mathbf{R}') = \int G(\tau_2, \mathbf{R}'', \mathbf{R}')G(\tau_1, \mathbf{R}, \mathbf{R}'')\mathrm{d}\mathbf{R}'', \tag{10}$$

allowing to express $G(\tau, \mathbf{R}, \mathbf{R}')$ in terms of short-time Green's functions $G(\Delta\tau, \mathbf{R}, \mathbf{R}')$ with $\Delta\tau \ll \tau$ for which accurate approximations, called short-time approximations, are available. A short-time approximation is mathematically the same as the high-temperature limit of statistical thermodynamics. Let $G^0(\Delta\tau, \mathbf{R}, \mathbf{R}')$ be a short-time approximation then

$$\begin{aligned} G(\tau, \mathbf{R}, \mathbf{R}') = \lim_{N\to\infty} & \int \mathrm{d}\mathbf{R}_{N-1} G^0(\Delta\tau, \mathbf{R}_{N-1}, \mathbf{R}') \\ & \times \int \mathrm{d}\mathbf{R}_{N-2} G^0(\Delta\tau, \mathbf{R}_{N-2}, \mathbf{R}_{N-1}) \cdots \\ & \cdots \int \mathrm{d}\mathbf{R}_1 G^0(\Delta\tau, \mathbf{R}_1, \mathbf{R}_2) G^0(\Delta\tau, \mathbf{R}, \mathbf{R}_1) \end{aligned} \tag{11}$$

with the time step $\Delta\tau = \tau/N$ and the number of time steps N.

The Trotter formula[9]

$$\mathrm{e}^{-\tau H} = \lim_{N\to\infty} \left(\mathrm{e}^{-\tau T}\mathrm{e}^{-\tau V}\right)^N$$

leads to a possible short-time approximation

$$G^0(\Delta\tau, \mathbf{R}, \mathbf{R}') = \langle \mathbf{R}'|\mathrm{e}^{-\Delta\tau T}|\mathbf{R}\rangle \mathrm{e}^{-V(\mathbf{R})\Delta\tau}, \tag{12}$$

where $G_\mathrm{d}(\tau, x, y) = \langle \mathbf{R}'|\mathrm{e}^{-\tau T}|\mathbf{R}\rangle$ is the known Green's function of the pure diffusion process

$$G_\mathrm{d}(\tau, \mathbf{R}, \mathbf{R}') = \frac{1}{\sqrt{2\pi\tau}} \mathrm{e}^{-\frac{(\mathbf{R}'-\mathbf{R})^2}{2\tau}}. \tag{13}$$

Usually, a more accurate symmetrical form

$$G^0(\tau, \mathbf{R}, \mathbf{R}') = G_\mathrm{d}(\tau, \mathbf{R}, \mathbf{R}')\mathrm{e}^{-\frac{1}{2}[V(\mathbf{R})+V(\mathbf{R}')]\tau}, \tag{14}$$

or other even more accurate forms are employed in DMC.[10, 11]

The exact solution including the exact ground state wavefunction as long-time stationary solution can now be expressed in terms of known short-time functions:

$$\begin{aligned} \psi(t, x) = \lim_{N\to\infty} & \int \mathrm{d}x_{N-1} G^0(\tau, x_{N-1}, x) \\ & \times \int \mathrm{d}x_{N-2} G^0(\tau, x_{N-2}, x_{N-1}) \cdots \\ & \cdots \int \mathrm{d}x_1 G^0(\tau, x_1, x_2) \\ & \times \int \mathrm{d}x_0 G^0(\tau, x_0, x_1)\phi_0(x_0). \end{aligned} \tag{15}$$

This representation of the wavefunction constitutes the connection to a Markov chain, or random walk process. Let X and Y be independent random variables with the probability density functions $p_X(x)$ and $p_Y(y)$. Probability density functions are nonnegative and normalized: $\phi_0(x) \geq 0$, $\int \mathrm{d}x\, \phi_0(x) = 1$. The random variable $Z = X + Y$ has the probability density

$$p_Z(z) = \int_\Omega p_Y(z - x)\, p_X(x)\mathrm{d}x, \tag{16}$$

where $p_Y(z - x)$ describes the transition probability to move from x to z as being independent of the position x.

Provided that the initial function ϕ_0 is a probability density and the short-time Green's function $G^0(\Delta\tau, x, y)$ a probability density of the form $p_\tau(y - x)$, such as G_d in Eq. (13), the solution $\psi(t, x)$ is the probability density of X_N defined by the stochastic process (or random walk process)

$$X_{k+1} = X_k + Y \tag{17}$$

with $X_0 \sim \phi_0(x)$, i.e., X_0 having the density ϕ_0. This equation defines one step of the random walk. Repeated simulation of the random walk for N steps yields a sample $\{\mathbf{R}_N^i\}_{i=1,\ldots,M}$ of $\psi_0(x)$ that can be used for calculating expectation values, i.e., integrals, over ψ_0.

The short-time approximation G^0 in Eq. (14) is not simply a probability density function but contains

 © 2011 John Wiley & Sons, Ltd.

17590884, 2011, 3, Downloaded from https://wires.onlinelibrary.wiley.com/doi/10.1002/wcms.40 by TEI of Greece, Wiley Online Library on [11/12/2025]. See the Terms and Conditions (https://onlinelibrary.wiley.com/terms-and-conditions) on Wiley Online Library for rules of use; OA articles are governed by the applicable Creative Commons License

an additional factor $e^{-\frac{1}{2}[V(\mathbf{R})+V(\mathbf{R}')]\tau}$. This factor can be treated as a weighting or branching factor.

This simple random walk approach is unfortunately numerically unstable for electronic structure problems because the additional factor fluctuates strongly due to the Coulomb potential and even has singularities. Numerically stable and efficient algorithms are obtained with the importance sampling transformation.[12, 13] Importance sampling makes use of a guide function $\phi_G(\mathbf{R})$ that is an approximation to the ground state wavefunction $\psi_0(\mathbf{R})$. It is usually of the same Slater–Jastrow form as the trial function in VMC, but it has a different role in DMC. ϕ_G is assumed to be real like all other wavefunctions in this advanced review. For the importance sampled DMC method, the operator $\tilde{H} = \phi(\mathbf{R})H\phi(\mathbf{R})^{-1} - E_{\text{ref}}$ is introduced, where E_{ref} is a reference energy that approximates the ground state energy E_0. $\tilde{H}$ is non-Hermitian and has the eigenfunctions $f_k(\mathbf{R}) = \psi_k(\mathbf{R})\phi_G(\mathbf{R})$ and the shifted eigenvalues $E_k - E_{\text{ref}}$. The function $f(\tau, \mathbf{R}) = \phi(\mathbf{R})\psi(\tau, \mathbf{R})$ solves the equation

$$\frac{\partial f}{\partial \tau} = -\tilde{H} f \tag{18}$$

with the initial condition $f(0, \mathbf{R}) = |\phi_G(\mathbf{R})|^2$. For the DMC random walk, a sample of the initial function $f(0, \mathbf{R})$ is required. This is easily obtained with a VMC run where the Metropolis–Hastings method generates the distribution $|\phi_G(\mathbf{R})|^2$ when $\phi_G \equiv \phi_T$.

The long-time limit of f is obviously

$$f(\tau, \mathbf{R}) \overset{\tau\to\infty}{\longrightarrow} \phi_G(\mathbf{R})\psi_0(\mathbf{R}). \tag{19}$$

After evaluation of $\phi_G \Delta \phi_G^{-1}$ one obtains

$$\frac{\partial f}{\partial \tau} = -Lf - (E_{\text{L}}(\mathbf{R}) - E_{\text{ref}})f \tag{20}$$

with the Fokker–Planck operator

$$L = -\frac{1}{2}\Delta + \nabla b(\mathbf{R}), \quad b(\mathbf{R}) = \frac{\nabla\phi(\mathbf{R})}{\phi(\mathbf{R})} \tag{21}$$

and the *local energy* $E_{\text{L}}(\mathbf{R}) = \phi(\mathbf{R})^{-1}H\phi(\mathbf{R})$.

The Green's function $G(\tau, \mathbf{R}, \mathbf{R}') = \langle \mathbf{R}'|e^{-\tilde{H}\tau}|\mathbf{R}\rangle$ is decomposed as before with

$$G^0(\tau, \mathbf{R}, \mathbf{R}') = G_{\text{dd}}(\tau, \mathbf{R}, \mathbf{R}') \cdot W(\tau, \mathbf{R}, \mathbf{R}'), \tag{22}$$

where

$$G_{\text{dd}}(\tau, \mathbf{R}, \mathbf{R}') = \frac{1}{\sqrt{2\pi\tau}} e^{-\frac{[\mathbf{R}'-(\mathbf{R}+b(\mathbf{R})\tau)]^2}{2\tau}},$$
$$W(\tau, \mathbf{R}, \mathbf{R}') = e^{-\left[\frac{1}{2}(E_{\text{L}}(\mathbf{R})+E_{\text{L}}(\mathbf{R}'))-E_{\text{ref}}\right]\tau}. \tag{23}$$

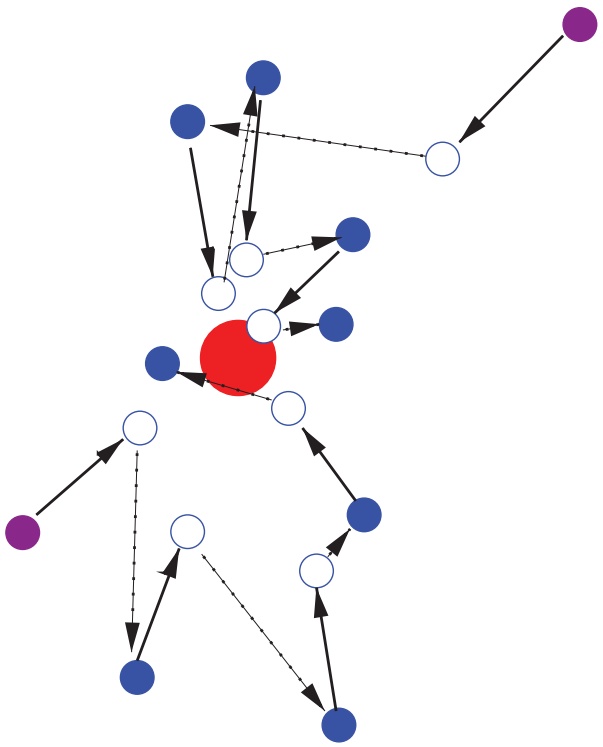

FIGURE 1 | Drift–diffusion process visualized for a Helium atom. The walker consists of the two electron positions. The initial walker is shown in violet, the following steps in blue. The drift toward the nucleus is shown as solid arrows, the intermediate position as hollow circles, and the random diffusion step with dotted arrows.

G_{dd} is a transition probability leading to the following *drift–diffusion process*

$$X_{k+1} = X_k + b(X_k)\tau + \Delta W_\tau \tag{24}$$

with $X_0 \sim \phi_G(\mathbf{R})^2$. ΔW_τ is a normal variate with $\mu = 0$ and $\sigma^2 = \tau$. The drift term $b(\mathbf{R}) = \nabla\phi_G/\phi_G$ causes the random walk to move away from small values of $|\phi_G|$ to large ones, therefore sampling the wavefunction where it is important. As ϕ_G 'guides' the random walk toward the important regions, it is usually called *guide function*. In Figure 1, the drift–diffusion process is visualized for the Helium atom.

As in the simple DMC algorithm, the weight $W(\tau, \mathbf{R}, \mathbf{R}')$ is treated as a weight of the walker or as a branching factor. The weighted probability density therefore represents $f(\tau, \mathbf{R})$ which converges with proper normalization in the long-time limit to

$$\bar{f}_\infty(\mathbf{R}) = \frac{\phi_G(\mathbf{R})\psi_0(\mathbf{R})}{\int \phi_G(\mathbf{R})\psi_0(\mathbf{R})d\mathbf{R}}. \tag{25}$$

This distribution is called the *mixed* distribution. It is used to obtain the DMC energy in the same way

© 2011 John Wiley & Sons, Ltd.

17590884, 2011, 3, Downloaded from https://wires.onlinelibrary.wiley.com/doi/10.1002/wcms.40 by TEI of Greece, Wiley Online Library on [11/12/2025]. See the Terms and Conditions (https://onlinelibrary.wiley.com/terms-and-conditions) on Wiley Online Library for rules of use; OA articles are governed by the applicable Creative Commons License

as the $|\phi_G|^2$ distribution is used to calculate the VMC energy:

$$E_{\mathrm{DMC}} = \frac{\int E_L(\mathbf{R})\phi_G(\mathbf{R})\psi_0(\mathbf{R})\mathrm{d}\mathbf{R}}{\int \phi_G(\mathbf{R})\psi_0(\mathbf{R})\mathrm{d}\mathbf{R}} = \lim_{M,N\to\infty} \frac{\sum_{i=1}^{M} w_N^i \cdot E_{\mathrm{L}}(\mathbf{R}_N^i)}{\sum_{i=1}^{M} w_N^i}. \quad (26)$$

The average is over the sample $\{\mathbf{R}_N^i\}_{i=1,M}$ at time step $N\Delta\tau$ obtained from the DMC random walk. Each walker has a weight w_N^i at time step $N\Delta\tau$ that might differ from one, depending on the specific algorithm to handle the weighting term $W(\tau, \mathbf{R}, \mathbf{R}')$. After stationarity has been reached the average can be carried out additionally over different time steps (i.e., N) as well. Because H is Hermitian the DMC mixed estimator yields the exact ground state energy within the statistical error bars

$$E_{\mathrm{DMC}} = \frac{\int E_{\mathrm{L}}(\mathbf{R})\phi_G(\mathbf{R})\psi_0(\mathbf{R})\mathrm{d}\mathbf{R}}{\int \phi_G(\mathbf{R})\psi_0(\mathbf{R})\mathrm{d}\mathbf{R}} = \frac{\int \phi_G(\mathbf{R})H\psi_0(\mathbf{R})\mathrm{d}\mathbf{R}}{\int \phi_G(\mathbf{R})\psi_0(\mathbf{R})\mathrm{d}\mathbf{R}} = E_0. \quad (27)$$

We are thus able to calculate the true ground state energy of H provided that $\phi_G(\mathbf{R})\psi(\tau, \mathbf{R})$ can be represented by a weighted density.

The energy is obtained as a weighted average of the local energy E_{L} over the random walker sample. The efficiency of the calculation is therefore determined by the time required to calculate E_{L}, the fluctuations of the weights, and the variance of the local energy $\sigma_{\mathrm{L}}^2 = \langle E_{\mathrm{L}}^2\rangle - \langle E_{\mathrm{L}}\rangle^2$.

The efficiency of this scheme can be improved considerably by adding a Metropolis-like acceptance step and branching[10, 13] or stochastic reconfiguration algorithms[14–16] that are not discussed here.

Fermion Sign Problem in Quantum Monte Carlo

The DMC method is an exact method (within statistical error bars) if $\phi_G(\mathbf{R})\psi_0(\mathbf{R})$ can be represented by a density. This is possible only if the guide function and the exact wavefunction have the same sign. Because electrons are fermions, the Pauli principle requires the electronic wavefunction to be antisymmetric. Therefore, all electronic wavefunctions (except for one and two electron ground states) have at least one positive and one negative domain. The product $\phi_G(\mathbf{R})\psi_0(\mathbf{R})$ can be a density only if ϕ_G has the same nodes as the exact wavefunction ψ_0 whose nodes are, in general, unknown like the function itself.

No accurate fermionic method is known that scales better with system size than exponentially. This is known as the sign problem. By 'accurate' we mean a method that calculates the energy of the system with a given accuracy (with respect to the exact solution of the Schrödinger equation). Accurate quantum Monte Carlo methods that scale exponentially are known, e.g., the released-node method[17] and the exact cancellation method.[18] Kalos and Pederiva[19] suggest a way to circumvent the sign problem with the fermion Monte Carlo method. This method is also discussed by Assaraf et al.[20] Recently, Troyer and Wiese[21] proved that the sign problem is nondeterministic polynomial (NP) hard meaning that a solution to the sign problem would provide a solution to other problems of complexity class NP as well. NP problems are those for which no algorithm is known that solves the problem in polynomial time on classical deterministic computers. Thus it is highly unlikely that a polynomial algorithm for the sign problem in QMC can be found and practical QMC methods for large systems will suffer from systematic errors. This is, in general, no problem as all electronic structure methods have systematic errors.

For the use in quantum chemistry, it is important to note that only *energy difference* such as reaction, excitation, or activation energies are of interest. While total energies may have a large error, it is necessary for the error of the energy difference to be of the order of chemical accuracy or 1 kcal/mol. In addition, it is desirable that a systematic improvement of the error is possible.

The sign problem is circumvented if the nodal surface of the electronic wavefunction is known in advance. The antisymmetry is built into the nodal surface and no sign change occurs within the domains D defined by the nodal surface. A systematic error, known as the node location error, arises when the nodal surface is not exact. In practice, an antisymmetric guide function ϕ_G is chosen, and its nodes $\phi_G = 0$ are taken as nodal surface for the electronic wavefunction ψ. The nodal surface is enforced in the quantum simulation by deletion or rejection of random walkers that cross a node, and, more efficiently, by construction of diffusion processes using importance sampling where the walkers do not cross the nodes in the limit of vanishing time steps τ. This is achieved with the drift–diffusion process and the drift term (cf. Eq. (24))

$$b(\mathbf{R})\tau = \frac{\nabla\phi_G(\mathbf{R})}{\phi(\mathbf{R})}\tau. \quad (28)$$

This method is known as fixed-node diffusion quantum Monte Carlo (FN-DMC).[22] The accuracy of the

17590884, 2011, 3, Downloaded from https://wires.onlinelibrary.wiley.com/doi/10.1002/wcms.40 by TEI of Greece, Wiley Online Library on [11/12/2025]. See the Terms and Conditions (https://onlinelibrary.wiley.com/terms-and-conditions) on Wiley Online Library for rules of use; OA articles are governed by the applicable Creative Commons License

FN-DMC method is thus determined by the accuracy of the nodes of the guide functions. The knowledge about the accuracy of the nodal surfaces of trial wavefunctions is therefore of great interest for the quantum Monte Carlo community.

Exact nodes are known only for a few systems. The lowest triplet state of the He atom has the node $r_1 = r_2$ which follows from the symmetry of the system. Mitas et al.[23, 24] have recently found exact nodes based on symmetry arguments for a number of high-spin systems. These nodes are very smooth and it has been suggested that the exact nodes are, in general, simpler and of higher symmetry than the corresponding wavefunctions.[25, 26] Bressanini and Reynolds[27] investigated in detail the nodes of the first excited singlet state of He and found a very simple node structure independent of the interelectronic angle θ_{12}. Very accurate Hylleraas calculations confirmed the simple structure, but found a very small, converged cosine-like dependence on θ_{12}.[28]

Pseudopotentials in Quantum Monte Carlo

Monte Carlo methods have the general property that they scale well with the system size. This holds, in general, also for the VMC and DMC methods when investigating hydrocarbons with increasing number of carbon atoms and thus electrons. The scaling of both methods with the nuclear charge Z is less favorable. It has been estimated as approximately $Z^{5.5-6.5}$, which is mainly due to the high kinetic energy of core electrons requiring increasingly small time steps.[4, 29] All-electron calculations beyond second-row elements are thus very demanding, and most of the simulation time is spent for the chemically inactive core electrons. Since the early days of quantum Monte Carlo, pseudopotentials have been used to eliminate the core electrons from the calculation.[30, 31] The same pseudopotentials as in standard calculations can be used in QMC, and the evaluation of the pseudopotentials in the context of QMC is well known. As in DFT or *ab initio* calculations, pseudopotentials also provide a simple and efficient way to include scalar relativistic effects into the electronic structure calculation. The effective Hamiltonian with pseudopotentials can be expressed as

$$H_{\text{eff}} = T + V_{\text{loc}} + W_{\text{nonloc}} \tag{29}$$

with the kinetic energy T of the valence electrons, a local potential V_{loc}, and a nonlocal potential W_{nonloc}. The latter is essential to retain orthogonality to the removed core states, but is difficult to implement in QMC. The standard way is the localization with the trial (or guide) wavefunction ϕ_T which introduces a small localization error that vanishes as the trial wavefunction becomes more accurate

$$W_{\text{loc}} = \frac{\int \phi_T^* W_{\text{nonloc}} \phi_T \mathrm{d}x}{\int \phi_T^* \phi_T \mathrm{d}x}. \tag{30}$$

The localization integral is usually calculated numerically.[32]

The standard pseudopotentials are not optimal for QMC calculations for several reasons. First, most standard pseudopotentials retain a singularity at the nucleus, which leads to large fluctuations of the local energy or even infinite variances in QMC. Second, the numerical integration of the nonlocal potential is expensive, and therefore it is desirable that the nonlocal potential decays quickly with increasing distance from the nucleus. Recently, soft pseudopotentials without singularities have been constructed by several groups specifically for QMC. Greeff and Lester[33] constructed HF-based pseudopotentials for the carbon atom, and Ovcharenko et al.[34] worked out pseudopotentials for most first- and second-row elements. Trail and Needs[35, 36] generated singularity-free relativistic pseudopotentials for most of the periodic table based on Dirac–Fock calculations. They included spin-orbit pseudopotentials, but no basis sets. Nonsingular energy-consistent scalar-relativistic HF pseudopotentials for the main group elements[37] and the 3d transition metals[38] have been designed by Burkatzki, Filippi, and Dolg. These authors provided efficient basis sets as well.

Casula[39] addressed the problem of the localization error in QMC and could demonstrate that parts of the nonlocal potential can be implemented quite simply in QMC. Badinski and Needs[40, 41] compared standard localized pseudopotentials with the semilocal form of Casula and found only a small effect.

Trial and Guide Functions in Quantum Monte Carlo

Both the VMC and the DMC method require an approximate wavefunction in analytic form, the trial and the guide function, respectively. The same types of function are used in both methods, and thus the function will be denoted simply by ϕ. It is important that only derivatives of ϕ are required, $\phi^{-1}\nabla\phi$ and $E_{\text{L}} = \phi^{-1}H\phi$ but no integrals. Because derivatives can always be calculated efficiently, compact wavefunctions that capture most of the many-electron physics can be employed.

The Slater–Jastrow function is the standard form for ϕ in QMC, a product of one or several Slater

© 2011 John Wiley & Sons, Ltd.

17590884, 2011, 3, Downloaded from https://wires.onlinelibrary.wiley.com/doi/10.1002/wcms.40 by TEI of Greece, Wiley Online Library on [11/12/2025]. See the Terms and Conditions (https://onlinelibrary.wiley.com/terms-and-conditions) on Wiley Online Library for rules of use; OA articles are governed by the applicable Creative Commons License

determinants ψ_n^{SD} and a Jastrow correlation function e^U:

$$\phi(x) = e^U \cdot \sum_n c_n \psi_n^{SD}. \quad (31)$$

It should be noted that the nodes, and thus the FN-DMC energy, depend only on the Slater determinant(s), but are independent of the Jastrow term. The VMC energies depend of course on the Jastrow term and on the Slater determinant.

The Slater determinants are often taken from HF, DFT, or complete active space (CASSCF) calculations. The construction of the Slater determinant from Kohn–Sham orbitals is particularly popular. The Jastrow correlation function e^U is often parametrized in the Schmidt–Moskowitz form,[42] where U is expanded in powers of the scaled distances $\bar{r}_i$ and $\bar{r}_{ij}$, $\bar{r} = r/(1 + ar)$. This expansion goes back to Boys and Handy.[43] Other expansions such as Padé-type[44, 45] or expansions in terms of unscaled distances with cutoff parameters[46] have been used successfully. The Jastrow factor does not have to be rotationally invariant. Riley and Anderson[47] demonstrated that a directional Jastrow term can improve the VMC energy of LiH considerably. The parameter vector $\mathbf{p}$ of $U(x, \mathbf{p})$ can be determined efficiently by minimizing the variance of the local energy in the form

$$\sigma_L^2 = \frac{1}{M} \sum_{i=1}^{M} (E_L(x_i, \mathbf{p}) - E_{ref})^2 \quad (32)$$

over a fixed sample $\{x_i\}_{i=1,\ldots,M}$ with the density $\phi(x, \mathbf{p}_0)^2$ obtained using the Metropolis–Hastings method and a reference energy $E_{ref} \approx \langle E_L \rangle$.[42, 48] It has been investigated several times how well the node location errors cancel when dissociation energies are calculated (see e.g., Refs 49 and 50).

In the last few years, a number of methods have been suggested that are able to optimize wavefunction parameters with respect to the VMC energy.[51–53] Particularly, successful methods are the effective fluctuation potential method by Filippi and Fahy,[54–58] the stochastic reconfiguration methods by Sorella et al.,[15, 59–63] and the linear optimization method by Toulouse and Umrigar.[64–67] A direct optimization of the FN-DMC energy is more complicated but limited progress has been achieved.[68–70]

For simulations of large molecules, the simple Slater–Jastrow form with one Slater determinant and a simple Jastrow correlation term are the most common. For smaller molecules, a number of more elaborate forms for the trial or guide function have been tested in the last few years with considerable success.

One way to increase the accuracy beyond simple FN-DMC is the use of more determinants. Efficient for reducing the node location error is the pair natural orbital configuration interaction (PNOCI) wavefunction as guide function.[71] CASSCF wavefunctions with large active spaces have been employed by Caffarel et al.[72–74] These authors emphasize the importance of systematic cancellation of the node location error which can be achieved with CASSCF-type wavefunctions.

A number of rather unusual types of wavefunctions have been used in QMC exploiting the flexibility of the ansatz without the necessity of integrals. The transcorrelated method, devised 40 years ago by Boys and Handy has been revived and extended with a simple Jastrow factor by Umezawa and Tsuneyuki.[75–79]

Expansion in terms of determinants is not the only way to represent accurate electronic wavefunctions. Recently, other types of functions have been employed in QMC calculations with great success. With only one pair function ϕ_g, a Bardeen, Cooper, Schrieffer (BCS) wavefunction, also known as antisymmetrized geminal power (AGP), is obtained

$$\Psi_{BCS} = \det(\phi_g(i, j)). \quad (33)$$

Functions of this type are successful in describing superconductivity, but can also be thought of as an extension of HF wavefunctions which are contained in Ψ_{BCS} as special case. This function has been introduced to QMC by Casula and Sorella[61, 62] who expanded the pair function into orbital products

$$\phi_g(i, j) = \sum_k \lambda_k \phi_k(r_i) \phi_k(r_j), \quad (34)$$

and combined it with a Jastrow function.

Functions of this type can be expressed efficiently in terms of Pfaffians, which can be calculated with the same effort as determinants. Recently, Mitas et al.[80, 81] explored the use of Pfaffians in VMC and DMC and obtained excellent results with one Pfaffian for small atoms and molecules with correlation energies of 94% and more.

The introduction of quasicoordinates that account for backflow is another method that is able to modify the nodal surface with a few parameters. The idea of backflow in a quantum system goes back to Feynman[82, 83] and was first introduced in the context of QMC by Lee et al.[84] Later, Ceperley et al.[85–88] extended the backflow idea to the homogeneous electron gas and the inhomogeneous systems liquid and solid hydrogen. Lopez Rios et al.[89] extended this approach further to atoms and molecules and were able to demonstrate the possibility to reduce the node location error with optimized quasicoordinates. In the

 © 2011 John Wiley & Sons, Ltd.

17590884, 2011, 3, Downloaded from https://wires.onlinelibrary.wiley.com/doi/10.1002/wcms.40 by TEI of Greece, Wiley Online Library on [11/12/2025]. See the Terms and Conditions (https://onlinelibrary.wiley.com/terms-and-conditions) on Wiley Online Library for rules of use; OA articles are governed by the applicable Creative Commons License

case of the carbon dimer C_2 these authors could improve the correlation energy from 92 to 95% of the exact value when switching from real to quasicoordinates in a Slater–Jastrow function. Drummond et al.[90] obtained 98% of the correlation energy of the Ne atom with one determinant and backflow coordinates. The computational cost of evaluating Slater determinants with quasicoordinates is increased because the coordinates depend on *all* electron coordinates r, but this cost might be offset by a reduced variance of the guide function. Backflow is therefore an efficient way of modifying the nodes. Gurtubay and Needs[91] obtained with one determinant and backflow almost the same DMC energy as Lüchow and Fink[71] with 300 determinants of a PNOCI expansion for the H_2O molecule. This demonstrates the effectiveness of the backflow guide functions in accounting for the influence of dynamic correlation on the nodal hypersurface.

Both the Pfaffian and the backflow approach toward more flexible but still efficient wavefunctions can easily be combined. Bajdich et al.[81] suggested this approach and found a significant, although small, improvement in the energy of the carbon dimer by adding backflow to the Pfaffian wavefunctions. These are very recent and somewhat preliminary results, and it is likely that even more flexible but still computationally efficient compact wavefunctions will be developed. It should be remarked that it is important to be able to systematically improve the percentage of correlation energy captured with DMC or VMC. On the other hand, it is even more important to obtain accurate energy *differences* than absolute energies for applications in chemistry. Therefore, the future focus will likely be on the construction of wavefunctions that allow a systematic cancellation of the node location error.

APPLICATIONS

Over the last years, quantum Monte Carlo has shown its ability for accurate calculations even in systems that are difficult for standard methods. In this section, we give an overview over some recent applications of QMC on molecular systems.

Transition Metal Compounds

Electronic structure calculations often become difficult when transition metals are involved. If the system has incomplete d shells, many electron configurations contribute even to the ground state leading to nondynamical electron correlation. Wavefunction-based methods with multideterminant references are required for high accuracy. Density functional theory calculations are often fairly accurate, but no current functional is reliable for transition metals compounds in general. QMC as a wavefunction-based method has to use multideterminant guide functions for very high accuracy but single determinant nodal surfaces based on Kohn–Sham orbitals often yield quite accurate results. Scalar relativistic effects are routinely included with pseudopotentials.

Wagner and Mitas[92, 93] calculated 3d transition metal monoxides with DMC and pseudopotentials using a single determinant based on B3LYP orbitals. The binding energy calculated with DMC is within the experimental error bars for ScO, TiO, and VO. The deviation for CrO and MnO is larger which indicates that a multideterminant approach might be necessary to account fully for the static electron correlation. In comparison with the coupled cluster method CCSD(T) and DFT with the Tao-Perdew-Staroverov-Scuseria hybrid functional (TPSSh) which performs particularly well for transition metals, DMC is the most accurate of all tested methods. Multideterminant FN-DMC calculations have been performed by Burkatzki et al.[38] using their soft pseudopotentials for ScO and TiO. These authors calculated the binding energy and the ionization potential and found a significant multireference effect.

Considerably larger transition metal compounds have been investigated by Diedrich et al.[94] with the neutral carbonyl complexes $Ni(CO)_4$, $Fe(CO)_5$, and $Cr(CO)_6$. Diedrich et al. calculated the dissociation energy for the abstraction of one carbon monoxide ligand using DMC with a single-determinant guide function and pseudopotentials on all atoms. Agreement with experimental data was achieved for the nickel and chromium complexes while the calculated value for the iron complex was less accurate. Bande and Lüchow[95] performed single-determinant DMC calculations on several neutral or cationic vanadium oxide molecules VO_n and VO_n^+ ($n = 1 - 4$) and V_2O_5. They employed pseudopotentials and compared Kohn–Sham orbitals from B3LYP and BP86 DFT calculations. The agreement with experimental ionization and oxygen abstraction energies where available was good with BP86 yielding slightly more accurate nodes for FN-DMC. El Akrimine et al.[96] modeled the chemisorption of CO on Cr(110) with a Cr_2 molecule and calculated with DMC the difference between the tilted and perpendicular orientations of CO.

Buendia et al.[97] calculated many states of the iron atom with VMC using orbitals obtained from the parametrized optimal effective potential method with all electrons included. Iron is a particularly

 © 2011 John Wiley & Sons, Ltd.

17590884, 2011, 3, Downloaded from https://wires.onlinelibrary.wiley.com/doi/10.1002/wcms.40 by TEI of Greece, Wiley Online Library on [11/12/2025]. See the Terms and Conditions (https://onlinelibrary.wiley.com/terms-and-conditions) on Wiley Online Library for rules of use; OA articles are governed by the applicable Creative Commons License

difficult system, and the VMC results are only moderately accurate. The same authors also published VMC and Green's functions quantum Monte Carlo (GFMC) calculations on the first transition-row atoms with all electrons.[98] GFMC is a variant of DMC where intermediate steps are used to remove the time-step error.

Caffarel et al.[99] presented a very careful study on the role of electron correlation and relativistic effects in the copper atom using all-electron FN-DMC. Relativistic effects were calculated with the Dirac–Fock model. Several states of the atom were evaluated and an accuracy of about 0.15 eV was achieved with a single determinant.

Excited States

VMC and DMC calculations are possible for excited states as well as for the ground state. In the case of FN-DMC, the nodal hypersurface of the guide function ϕ_G prohibits the relaxation of the system to the ground state. This is not really different from ground state calculations where the nodes prohibit the system to relax to the physically forbidden bosonic state. Excited state calculated with QMC thus require the guide functions ϕ_G to be built from an excited state wavefunction such as CIS or CASSCF.

Schautz and Filippi[57, 100] calculated excitation energies for small molecules, such as ethene, formaldehyde, and formaldimine, and obtained excellent agreement with experiment. These authors investigated in detail the influence of different types of guide wavefunctions on excitation energies and the twisting of the double bond. For $\pi \rightarrow \pi^*$ and $n \rightarrow \pi^*$ excitations in formaldehyde and formaldimine, respectively, very good agreement with experimental values was obtained with single-determinant guide function for the S_0 state and a two-determinant guide function for the S_1 state. The orbitals were optimized with the energy fluctuation potential method. State-averaged CASSCF wavefunctions were employed as well, in particular for the twisting of the double bond. The number of determinants in the FN-DMC or VMC calculations was restricted by using only determinants with a CI coefficient below a given threshold. The authors extended their study to the protonated imine $CH_2{=}CH{-}CH{=}CH{-}CH{=}NH_2^+$ which can be considered as a model for retinal, the chromophore in rhodopsin. Rhodopsin is involved in the primary step of vision as light induces a cis-trans isomerization of retinal. Schautz and Filippi[100] investigated this photoisomerization for the model iminium cation using FN-DMC with a guide wavefunction built from a state-averaged CASSCF wavefunction with the six π electrons distributed in the six π orbitals. Their FN-DMC result is close to accurate multi reference CI calculations but deviates strongly from simpler restricted open shell Kohn–Sham DFT results.

Bouabça et al.[73] investigated carefully the singlet $n \rightarrow \pi^*$ transition of acrolein, $CH_2{=}CH{-}CH{=}O$. They obtained good agreement with experiment using state-averaged CASSCF wavefunctions supplemented with a Jastrow factor as guide functions. Again, the multireference nature of the excited state made it necessary to employ the large active space CAS(6,5) to obtain converged results while the smaller CAS(2,2) with only the n and π^* orbital displayed a strong basis set dependency. The methodology is distinct from the work by Schautz and Filippi because Bouabça et al. do not optimize the wavefunction, only the Jastrow part of the wavefunction which does not change the nodes and therefore not the FN-DMC energy. They argue that retaining the orbitals and CI coefficients, in particular from a state averaged CASSCF calculation, enhances the necessary error cancellation for the excitation energy.

Singlet-triplet excitations have been calculated by Grossman et al.[101] for methane and silane and by El Akrimine et al.[102] for ethene. Bande et al.[103, 104] investigated Rydberg excitations of carbon monoxide and the carbon atom with DMC using only one configuration state function from open-shell localized Hartree–Fock calculations. Very accurate calculations by Zimmermann et al.[105] on the ground and several low-lying excited states of methylene are available with DMC where CAS wavefunctions with parameter optimizations are employed.

While these studies involve rather small molecules, the favorable scaling behavior of DMC and VMC can be exploited for the calculation of excitation energies in larger molecules. One example is the calculation of the excitation energies in the free base porphyrin, $C_{20}N_4H_{14}$. Porphyrins are a biologically very important class of molecules. Heme is a porphyrin with iron as central atom, playing a central role in biological oxygen transport, whereas chlorophyll contains a porphyrin variant with a magnesium atom at the center. Aspuru-Guzik et al.[106] calculated the vertical and adiabatic excitation energies to the first excited singlet and triplet species. With 11 conjugated double bonds it is currently impossible to carry out CASSCF calculation or to employ a many-determinant guide function in QMC. The guide functions for the DMC are simply HF wavefunctions with a simple Jastrow factor. Nonetheless, accuracy better then 0.1 eV is obtained for both the singlet and the triplet when the calculated energies are compared to experiment.

 © 2011 John Wiley & Sons, Ltd.

17590884, 2011, 3, Downloaded from https://wires.onlinelibrary.wiley.com/doi/10.1002/wcms.40 by TEI of Greece, Wiley Online Library on [11/12/2025]. See the Terms and Conditions (https://onlinelibrary.wiley.com/terms-and-conditions) on Wiley Online Library for rules of use; OA articles are governed by the applicable Creative Commons License

Another application of QMC to biologically important chromophores is a very recent study on a green fluorescent protein (GFP) chromophore by Filippi et al.[107] They studied *p*-hydroxybenzylideneimidazolinone and a few variants as GFP chromophore with VMC and DMC. They have been able to use CASSCF-type guide functions up to active spaces with 10 electrons in 10 orbitals, although with thresholds to keep the number of configuration state functions for QMC below 100. At least CAS(6,6) was necessary to obtain converged results. This highlights the importance of many-determinant guide functions to fully account for nondynamical correlation. These results also show how FN-DMC calculations with a single-determinant guide function can be improved systematically.

Drummond et al.[108] investigated the electron emission from diamondoids with DMC. Using DFT orbitals in DMC, they calculated the excitation energy for the optical gap, the electron affinity, and the ionization potential for carbon clusters with diamond structure up to $C_{87}H_{76}$.

The favorable scaling of DMC with the system size makes even calculations on surface models possible. Examples are calculations on a model of the silicon (100) surface ($Si_{21}H_{20}$) by Healy et al.[109] The same authors investigated the H_2 dissociation on a silicon (001) surface with silicon models up to $Si_{27}H_{24}$. They calculated adsorption, reaction, and desorption energies for different mechanisms.[110] More recently, Cicero et al.[111] calculated the adhesion of O_2 on single-walled carbon nanotubes with QMC.

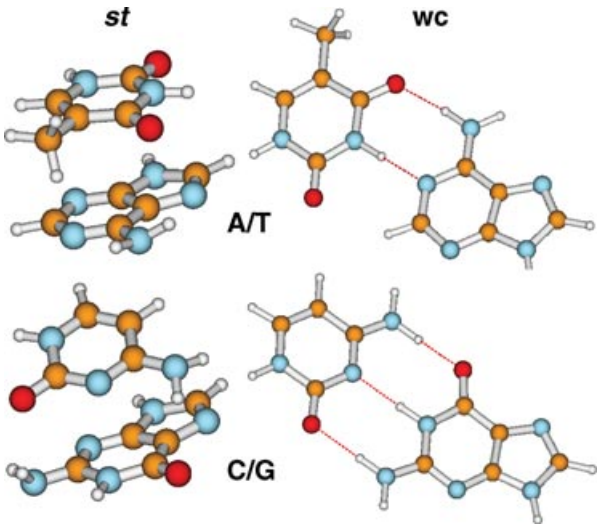

FIGURE 2 | Adenine/thymine and cytosine/guanine base pairs as calculated with fixed-node diffusion quantum Monte Carlo. The bases can interact via hydrogen bonding (Watson–Crick, wc) or via a π-stacking conformation (st). (Reprinted with permission from Ref 115. Copyright 2008 American Chemical Society.)

TABLE 1 | Binding Energies for DNA Base Pairs in the Watson–Crick Hydrogen-Bonded Arrangement (wc) and the π-stacking Arrangement (st)

	FN-DMC	est. CCSD(T)
Adenine–thymine (wc)	15.7(9)	15.4
Adenine–thymine (st)	13.1(8)	11.6
Cytosine–guanine (wc)	30.2(9)	28.8
Cytosine–guanine (st)	19.6(9)	16.9

Intermolecular Interactions

The accurate calculation of intermolecular interactions is the final type of applications to be discussed in this review. It is well known that HF and most DFT methods fail to describe van der Waals interactions even qualitatively correct while MP2 often overestimates this interaction. As an accurate method for electron correlation, DMC is expected to be well suited for intermolecular interactions, including weak interactions.

Very accurate calculations of the dissociation energy of the water dimer were performed by Needs et al.[91, 112] These authors did calculations with all electrons and with pseudopotentials and found very little effect of the pseudopotential approximation.

Diedrich et al.[113] could demonstrate with calculations on the dimers of methane, ammonia, and water, as well as the benzene dimer, that DMC performs very well on the whole range of interactions from pure dispersive to mainly electrostatic. They used pseudopotentials and HF orbitals. With a similar approach, Korth et al.[115] calculated the full S22 test set of dimers.[114] The benchmark calculations revealed a mean absolute deviation for the binding energy of only 0.68 kcal/mol. These authors also investigated the intermolecular bonding of DNA base pairs. The DNA bases adenine (A), thymine (T), cytosine (C), and guanine (G) can pair via hydrogen bonds to form the Watson–Crick pairs A–T or C–G, but they also show a π-stacking interaction (see Figure 2). In DNA, this interaction is important along the DNA strand. It is due to the attractive interaction of the π systems. The relative strength of π and hydrogen interaction is important for the stability of the double helix. Korth et al. calculated the interaction energies for both types of interaction and compared their values with extrapolated CCSD(T) data from Jurecka and Hobza[116] (see Table 1). The DMC energies are within the estimated uncertainty of 1–2 kcal/mol of

© 2011 John Wiley & Sons, Ltd.

17590884, 2011, 3, Downloaded from https://wires.onlinelibrary.wiley.com/doi/10.1002/wcms.40 by TEI of Greece, Wiley Online Library on [11/12/2025]. See the Terms and Conditions (https://onlinelibrary.wiley.com/terms-and-conditions) on Wiley Online Library for rules of use; OA articles are governed by the applicable Creative Commons License

the extrapolated CCSD(T) values. The DMC calculations do not rely on any extrapolation. The data show that the π stacking interaction for A–T pair is almost as strong as the hydrogen bonded interaction. The hydrogen bond energy for the C–G pair is considerably stronger than the corresponding π interaction because C–G is bound by three hydrogen bonds, whereas the A–T Watson–Crick pair has only two hydrogen bonds. Overall, the DMC calculations confirm the strong interaction of the π systems along the DNA strands and their importance for the stability of the double helix structure.

Very accurate results for the parallel displaced benzene dimer were obtained by Sorella et al.[117] who obtained a binding energy of 2.2 kcal/mol. These authors used their AGP approach with a Jastrow function and carefully optimized wavefunction parameters.

DMC calculations begin to play a role in supermolecular chemistry. Very recently Zaccheddu et al.[118] calculated the anion-π interaction of triazine nitrate complexes and triazine dimers with DMC and analyzed the cooperative effects for the self-assembly. In this study, the Burkatzki pseudopotentials were used, and the wavefunction parameters were optimized using VMC minimization.

CONCLUSION AND OUTLOOK

Over the last decade, it could be demonstrated that high accuracy for fairly large molecular systems can be achieved with the latest developments in QMC methodology. In this review, applications to systems that are difficult for quantum chemistry in general have been presented. In particular, the DMC method could show its capability of calculating accurately transition metal compounds, excited states, and the interaction energy of weakly bound systems. Although QMC calculations remain time-consuming, they can be readily adapted to massively parallel computers. Because the hardware technology has been shifting from increasing CPU speed to integrating more processor cores into a single processor, the development of the next generations of computers will allow accurate QMC calculations on even larger systems than today.

REFERENCES

1. Lester WA, Mitas L, Hammond B. Quantum Monte Carlo for atoms, molecules and solids. *Chem Phys Lett* 2009, 478:1.
2. Aspuru-Guzik A, Lester WA. Quantum Monte Carlo: theory and application to molecular systems. *Adv Quant Chem* 2005, 49:209.
3. Lüchow A, Anderson JB. Monte Carlo methods in electronic structure for large systems. *Annu Rev Phys Chem* 2000, 51:501.
4. Hammond BL, Lester WA, Reynolds PJ. *Monte Carlo Methods in Ab Initio Quantum Chemistry*. World Scientific: Singapore; 1994.
5. Schrödinger E. Über die Umkehrung der Naturgesetze. *Sitzber Preuss Akad Wiss Phys-Math Kl* 1931, 144.
6. Anderson JB. *Quantum Monte Carlo: Origins, Developments, Applications*. Oxford University Press; 2007.
7. Metropolis N, Rosenbluth AW, Rosenbluth MN, Teller AM, Teller E. Equation of state calculations by fast computing machines. *J Chem Phys* 1953, 21:1087.
8. Hastings WK. Monte Carlo sampling methods using Markov chains and their applications. *Biometrika* 1970, 57:97.
9. Trotter H. On the product of semigroups of operators. *Proc Amer Math Soc* 1959, 10:545.
10. Umrigar CJ, Nightingale MP, Runge KJ. A diffusion Monte Carlo algorithm with very small time step errors. *J Chem Phys* 1993, 99:2865.
11. Håkansson P, Mella M, Bressanini D, Morosi G, Patrone M. Improved diffusion Monte Carlo propagators for bosonic systems using Itô calculus. *J Chem Phys* 2006, 125:184106.
12. Grimm RC, Storer RG. Monte-Carlo Solution of Schroedinger's equation. *J Comp Phys* 1971, 7: 134.
13. Reynolds PJ, Ceperley DM, Alder B, Lester WA. Fixed-node quantum Monte Carlo for molecules. *J Chem Phys* 1982, 77:5593.
14. Hetherington JH. Observations on the statistical iteration of matrices. *Phys Rev* A 1984, 30: 2713.
15. Calandra Buonaura M, Sorella S. Numerical study of the two-dimensional Heisenberg model using a Green function Monte Carlo technique with a fixed number of walkers. *Phys Rev B* 1998, 57:11446.
16. Assaraf R, Caffarel M, Khelif A. Diffusion Monte Carlo methods with a fixed number of walkers. *Phys Rev E* 2000, 61:4566.

 © 2011 John Wiley & Sons, Ltd.

17590884, 2011, 3, Downloaded from https://wires.onlinelibrary.wiley.com/doi/10.1002/wcms.40 by TEI of Greece, Wiley Online Library on [11/12/2025]. See the Terms and Conditions (https://onlinelibrary.wiley.com/terms-and-conditions) on Wiley Online Library for rules of use; OA articles are governed by the applicable Creative Commons License

17. Ceperley DM, Alder BJ. Quantum Monte Carlo for molecules—Green's function and nodal release. *J Chem Phys* 1984, 81:5833.
18. Anderson JB, Traynor CA, Boghosian BM. An exact quantum Monte Carlo calculation of the helium–helium intermolecular potential. *J Chem Phys* 1993, 99:345.
19. Kalos MH, Pederiva F. Exact Monte Carlo method for continuum fermion systems. *Phys Rev Lett* 2000, 85:3547.
20. Assaraf R, Caffarel M, Khelif A. The fermion Monte Carlo revisited. *J Phys A: Math Theor* 2007, 40: 1181.
21. Troyer M, Wiese UJ. Computational complexity and fundamental limitations to fermionic quantum monte carlo simulations. *Phys Rev Lett* 2005, 94:170201.
22. Anderson JB. Quantum chemistry by random walks. *J Chem Phys* 1976, 65:4121.
23. Bajdich M, Mitas L, Drobny G, Wagner LK. Approximate and exact nodes of fermionic wavefunctions: coordinate transformations and topologies. *Phys Rev B* 2005, 72:075131.
24. Mitas L. Structure of fermion nodes and nodal cells. *Phys Rev Lett* 2006, 96:240402.
25. Bressanini D, Ceperley DM, Reynolds PJ. What do we know about wave function nodes. In: Lester WA, Rothstein SM, Tanaka S, eds. *Recent advances in Quantum Monte Carlo methods, Part II*. World Scientific: Singapore; 2002.
26. Bressanini D, Morosi G, Tarasco S. An investigation of nodal structures and the construction of trial wave functions. *J Chem Phys* 2005, 123:204109.
27. Bressanini D, Reynolds PJ. Unexpected symmetry in the nodal structure of the He atom. *Phys Rev Lett* 2005, 95:110201.
28. Scott TC, Lüchow A, Bressanini D, J D Morgan I. The nodal surfaces of helium atom eigenfunctions. *Phys Rev* A 2007, 75:060101R.
29. Ceperley DM. The statistical error of Green's function Monte Carlo. *J Stat Phys* 1986, 43:815.
30. Hurley MM, Christiansen PA. Relativistic effective potentials in quantum Monte Carlo calculations. *J Chem Phys* 1987, 86:1069.
31. Hammond BL, Reynolds PJ, Lester WA. Valence quantum Monte Carlo with ab initio effective core potentials. *J Chem Phys* 1987, 87:1130.
32. Mitas L, Shirley EL, Ceperley DM. Nonlocal pseudopotentials and diffusion Monte Carlo. *J Chem Phys* 1991, 95:3467.
33. Greeff CW, Lester WA. A soft Hartree-Fock pseudopotential for carbon with application to quantum Monte Carlo. *J Chem Phys* 1998, 109:1607.
34. Ovcharenko I, Aspuru-Guzik A, Lester WA. Soft pseudopotentials for efficient quantum Monte Carlo calculations: from Be to Ne and Al to Ar. *J Chem Phys* 2001, 114:7790.
35. Trail JR, Needs RJ. Norm-conserving Hartree-Fock pseudopotentials and their asymptotic behavior. *J Chem Phys* 2005, 122:014112.
36. Trail JR, Needs RJ. Smooth relativistic Hartree-Fock pseudopotentials for H to Ba and Lu to Hg. *J Chem Phys* 2005, 122:174109.
37. Burkatzki M, Filippi C, Dolg M. Energy-consistent pseudopotentials for quantum Monte Carlo calculations. *J Chem Phys* 2007, 126:234105.
38. Burkatzki M, Filippi C, Dolg M. Energy-consistent small-core pseudopotentials for 3d-transition metals adapted to quantum Monte Carlo calculations. *J Chem Phys* 2008, 129:164115.
39. Casula M. Beyond the locality approximation in the standard diffusion Monte Carlo method. *Phys Rev B* 2006, 74:161102.
40. Badinski A, Needs RJ. Accurate forces in quantum Monte Carlo calculations with nonlocal pseudopotentials. *Phys Rev E* 2007, 76:036707.
41. Badinski A, Needs RJ. Total forces in the diffusion Monte Carlo method with nonlocal pseudopotentials. *Phys Rev B* 2008, 78:035134.
42. Schmidt KE, Moskowitz JW. Correlated Monte Carlo wave functions for the atoms He through Ne. *J Chem Phys* 1990, 93:4172.
43. Boys SF, Handy NC. A calculation for the energies and wavefunctions for states of neon with full electronic correlation accuracy. *Proc R Soc Lond Ser A* 1969, 310:63.
44. Umrigar CJ, Wilson KG, Wilkins JW. A method for determining many-body wave functions. In: Landau DP, Mon KK, Schüttler H, eds. *Computer Simulation Studies in Condensed Matter Physics: Recent Developments*. Heidelberg: Springer; 1988.
45. Umrigar CJ, Wilson KG, Wilkins JW. Optimized trial wave functions for quantum Monte Carlo calculations. *Phys Rev Lett* 1988, 60:1719.
46. Drummond ND, Towler MD, Needs RJ. Jastrow correlation factor for atoms, molecules, and solids. *Phys Rev B* 2004, 70:235119.
47. Riley KE, Anderson JB. A new variational Monte Carlo trial wave function with directional Jastrow functions. *Chem Phys Lett* 2002, 366:153.
48. Kent PRC, Needs RJ, Rajagopal G. Monte Carlo energy and variance-minimization techniques for optimizing many-body wave functions. *Phys Rev B* 1999, 59:12344.
49. Lüchow A, Anderson JB. First-row hydrides: dissociation and ground state energies using quantum Monte Carlo. *J Chem Phys* 1996, 105:7573.
50. Grossman JC. Benchmark quantum Monte Carlo calculations. *J Chem Phys* 2002, 117:1434.
51. Snajdr M, Dwyer JR, Rothstein SM. Histogram filtering: a technique to optimize wave functions for use in Monte Carlo simulations. *J Chem Phys* 1999, 111:9971.

 © 2011 John Wiley & Sons, Ltd.

17590884, 2011, 3, Downloaded from https://wires.onlinelibrary.wiley.com/doi/10.1002/wcms.40 by TEI of Greece, Wiley Online Library on [11/12/2025]. See the Terms and Conditions (https://onlinelibrary.wiley.com/terms-and-conditions) on Wiley Online Library for rules of use; OA articles are governed by the applicable Creative Commons License

52. Snajdr M, Dwyer JR, Rothstein SM. Erratum: "Histogram filtering—a technique to optimize wave functions for use in Monte Carlo simulations" [*J Chem Phys* 1999, 111:9971]. *J Chem Phys* 2001, 114:6960.
53. Lin X, Zhang H, Rappe AM. Optimization of quantum Monte Carlo wave functions using analytical energy derivatives. *J Chem Phys* 2000, 112:2650.
54. Filippi C, Fahy S. Optimal orbitals from energy fluctuations in correlated wave functions. *J Chem Phys* 2000, 112:3523.
55. Prendergast D, Bevan D, Fahy S. Optimization of inhomogeneous electron correlation factors in periodic solids. *Phys Rev B*. 2002, 66:155104.
56. Schautz F, Fahy S. Optimization of configuration interaction coefficients in multideterminant Jastrow–Slater wave functions. *J Chem Phys* 2002, 116:3533.
57. Schautz F, Filippi C. Optimized Jastrow Slater wave functions for ground and excited states: application to the lowest states of ethene. *J Chem Phys* 2004, 120:10931.
58. Scemama A, Filippi C. Simple and efficient approach to the optimization of correlated wave functions. *Phys Rev B* 2006, 73:241101.
59. Sorella S. Green function Monte Carlo with stochastic reconfiguration. *Phys Rev Lett* 1998, 80:4558.
60. Sorella S. Generalized Lanczos algorithm for variational quantum Monte Carlo. *Phys Rev B*. 2001, 64:024512.
61. Casula M, Sorella S. Geminal wave functions with Jastrow correlation: a first application to atoms. *J Chem Phys* 2003, 119:6500.
62. Casula M, Attaccalite C, Sorella S. Correlated geminal wave function for molecules: an efficient resonating valence bond approach. *J Chem Phys* 2004, 121:7110.
63. Sorella S. Wave function optimization in the variational Monte Carlo method. *Phys Rev B*. 2005, 71:241103.
64. Nightingale MP, Melik-Alaverdian V. Optimization of ground- and excited-state Wave Functions and van der Waals clusters. *Phys Rev* L. 2001, 87:043401.
65. Umrigar CJ, Toulouse J, Filippi C, Sorella S, Henning RG. Alleviation of the fermion-sign problem by optimization of many-body wave functions. *Phys Rev Lett* 2007, 98:110201.
66. Toulouse J, Umrigar CJ. Optimization of quantum Monte Carlo wave functions by energy minimization. *J Chem Phys* 2007, 126:084102.
67. Toulouse J, Umrigar CJ. Full optimization of Jastrow–Slater wave functions with application to the first-row atoms and homonuclear diatomic molecules. *J Chem Phys* 2008, 128:174101.
68. Reboredo FA, Kent PRC. Density–density functionals and effective potentials in many-body electronic structure calculations. *Phys Rev B* 2008, 77:245110.
69. Lüchow A, Scott TC. Nodal structure of Schrödinger wave function: general results and specific models. *J Phys* B 2007, 40:851.
70. Lüchow A, Petz R, Scott TC. Direct optimization of nodal hypersurfaces in approximate wave functions. *J Chem Phys* 2007, 126:144110.
71. Lüchow A, Fink RF. On the systematic improvement of fixed-node diffusion quantum Monte Carlo energies using pair natural orbital CI guide functions. *J Chem Phys* 2000, 113:8457.
72. Caffarel M, Hernandez-Lamoneda R, Scemama A, Ramírez-Solís A. Multireference quantum Monte Carlo study of the O_4 molecule. *Phys Rev Lett* 2007, 99:153001.
73. Bouabça T, Amor NB, Maynau D, Caffarel M. A study of the fixed-node error in quantum Monte Carlo calculations of electronic transitions: The case of the singlet n→ π^* (CO) transition of the acrolein. *J Chem Phys* 2009, 130:114107.
74. Scemama A, Caffarel M, Ramírez-Solís A. Bond breaking and bond making in tetraoxygen: analysis of the O_2 ($X^3\Sigma_g^-$) + O_2 ($X^3\Sigma_g^-$) → O_4 reaction using the electron pair localization function. *J Phys Chem* A 2009, 113:9014.
75. Umezawa N, Tsuneyuki S. Transcorrelated method for electronic systems coupled with variational Monte Carlo calculation. *J Chem Phys* 2003, 119:10015.
76. Umezawa N, Tsuneyuki S. Excited electronic state calculations by the transcorrelated variational Monte Carlo method: application to a helium atom. *J Chem Phys* 2004, 121:7070.
77. Umezawa N, Tsuneyuki S, Ohno T, Shiraishi K, Chikyow T. A practical treatment for the three-body interactions in the transcorrelated variational Monte Carlo method: application to atoms from lithium to neon. *J Chem Phys* 2005, 122:224101.
78. Umezawa N, Chikyow T. Role of the one-body Jastrow factor in the transcorrelated self-consistent field equation. *Int J Quantum Chem* 2006, 106:1477.
79. Prasad R, Umezawa N, Domin D, Salomon-Ferrer R, Lester WA. Quantum Monte Carlo study of first-row atoms using transcorrelated variational Monte Carlo trial functions. *J Chem Phys* 2007, 126:164109.
80. Bajdich M, Mitas L, Drobny G, Wagner LK, Schmidt KE. Pfaffian pairing wave functions in electronic-structure quantum Monte Carlo simulations. *Phys Rev Lett* 2006, 96:130201.
81. Bajdich M, Mitas L, Wagner LK. Pfaffian pairing and backflow wavefunctions for electronic structure quantum Monte Carlo methods. *Phys Rev B* 2008, 77:115112.
82. Feynman R. Atomic theory of the two-fluid Model of liquid helium. *Phys Rev* 1954, 94:262.
83. Feynman R, Cohen M. Energy spectrum of the excitations in liquid Helium. *Phys Rev* 1956, 102:1189.

 © 2011 John Wiley & Sons, Ltd.

17590884, 2011, 3, Downloaded from https://wires.onlinelibrary.wiley.com/doi/10.1002/wcms.40 by TEI of Greece, Wiley Online Library on [11/12/2025]. See the Terms and Conditions (https://onlinelibrary.wiley.com/terms-and-conditions) on Wiley Online Library for rules of use; OA articles are governed by the applicable Creative Commons License

84. Lee MA, Schmidt KE, Kalos MH, Chester GV. Green's function Monte Carlo method for liquid 3He. *Phys Rev Lett* 1981, 46:728.
85. Kwon Y, Ceperley DM, Martin RM. Effects of three-body and backflow correlations in the two-dimensional electron gas. *Phys Rev B* 1993, 48:12037.
86. Kwon Y, Ceperley DM, Martin RM. Effects of backflow correlation in the three-dimensional electron gas: quantum Monte Carlo study. *Phys Rev B* 1998, 58:6800.
87. Holzmann M, Ceperley DM, Pierleoni C, Esler K. Backflow correlations for the electron gas and metallic hydrogen. *Phys Rev E* 2003, 68:46707.
88. Pierleoni C, Ceperley DM, Holzmann M. Coupled electron-ion Monte Carlo calculations of dense metallic hydrogen. *Phys Rev Lett* 2004, 93:146402.
89. Rios PL, Ma A, Drummond ND, Towler MD, Needs RJ. Inhomogeneous backflow transformations in quantum Monte Carlo calculations. *Phys Rev E* 2006, 74:066701.
90. Drummond ND, Rios PL, Ma A, Trail JR, Spink GG, Towler MD, Needs RJ. Quantum Monte Carlo study of the Ne atom and the Ne+ ion. *J Chem Phys* 2006, 124:224104.
91. Gurtubay IG, Needs RJ. Dissociation energy of the water dimer from quantum Monte Carlo calculations. *J Chem Phys* 2007, 127:124306.
92. Wagner L, Mitas L. A quantum Monte Carlo study of electron correlation in transition metal oxygen molecules. *Chem Phys Lett* 2003, 370:412.
93. Wagner LK, Mitas L. Energetics and dipole moment of transition metal monoxides by quantum Monte Carlo. *J Chem Phys* 2007, 126:034105.
94. Diedrich C, Lüchow A, Grimme S. Performance of the diffusion Monte Carlo method for the first dissociation energies of transition metal carbonyls. *J Chem Phys* 2005, 122:21101.
95. Bande A, Lüchow A. Vanadium oxide compounds with quantum Monte Carlo. *Phys Chem Chem Phys* 2008, 10:3371.
96. Akramine OE, Lester WA, Krokidis X, Taft CA, Guimaraes TC, Pavao AC, Zhu R. Quantum Monte Carlo study of the CO interaction with a dimer model surface for Cr(110). *Mol Phys* 2003, 101:277.
97. Buendía E, Gálvez FJ, Sarsa A. Correlated wave functions for the ground and some excited states of the iron atom. *J Chem Phys* 2006, 124:154101.
98. Sarsa A, Buendía E, Gálvez FJ, Maldonado P. Quantum Monte Carlo for 3d transition-metal atoms. *J Phys Chem A* 2008, 112:2074.
99. Caffarel M, Daudey JP, Heully JL, Ramirez-Solis A. Towards accurate all-electron quantum Monte Carlo calculations of transition-metal systems: spectroscopy of the copper atom. *J Chem Phys* 2005, 123:094102.
100. Schautz F, Buda F, Filippi C. Excitations in photoactive molecules from quantum Monte Carlo. *J Chem Phys* 2004, 121:5836.
101. Grossman JC, Rohlfing M, Mitas L, Louie SG, Cohen ML. High accuracy many-body calculational approaches for excitations in molecules. *Phys Rev Lett* 2001, 86:472.
102. Akramine OE, Kollias AC, Lester WA. Quantum Monte Carlo study of singlet-triplet transitions in ethylene. *J Chem Phys* 2003, 119:1483.
103. Bande A, Lüchow A, Della Sala F, Görling A. Rydberg states with quantum Monte Carlo. *J Chem Phys* 2006, 124:114114.
104. Bande A, Lüchow A. Rydberg states with quantum Monte Carlo. In: Anderson JB, Rothstein S, eds. *Recent Advances in Quantum Monte Carlo*. Washington, DC: ACS Proceedings; 2007.
105. Zimmerman PM, Toulouse J, Zhang Z, Musgrave CB, Umrigar CJ. Excited states of methylene from quantum Monte Carlo. *J Chem Phys* 2009, 131:124103.
106. Aspuru-Guzik A, Akramine OE, Grossman JC, Lester WA. Quantum Monte Carlo for electronic excitations of free-base porphyrin. *J Chem Phys* 2004, 120:3049.
107. Filippi C, Zaccheddu M, Buda F. Absorption Spectrum of the Green fluorescent protein chromophore: a difficult case for ab initio methods? *J Chem Theory Comput* 2009, 5:2074.
108. Drummond ND, Williamson AJ, Needs RJ, Galli G. Electron emission from diamondoids: a diffusion quantum Monte Carlo study. *Phys Rev Lett* 2005, 95:096801.
109. Healy SB, Filippi C, Kratzer P, Penev E, Scheffler M. Role of electronic correlation in the Si(100) reconstruction: a quantum Monte Carlo study. *Phys Rev Lett* 2001, 87:016105.
110. Filippi C, Healy SB, Kratzer P, Pehlke E, Scheffler M. Quantum Monte Carlo calculations of H_2 dissociation on Si(001). *Phys Rev Lett* 2002, 89:166102.
111. Cicero G, Grossmann JC, Galli G. Adhesion of single functional groups to individual carbon nanotubes: electronic effects probed by ab initio calculations. *Phys Rev B* 2006, 74:035425.
112. Benedek NA, Snook IK, Towler MD, Needs RJ. Quantum Monte Carlo calculations of the dissociation energy of the water dimer. *J Chem Phys* 2006, 125:104302.
113. Diedrich C, Lüchow A, Grimme S. Weak intermolecular interactions calculated with diffusion Monte Carlo. *J Chem Phys* 2005, 123:184106.
114. Jurecka P, Sponer J, Cerny J, Hobza P. Benchmark database of accurate (MP2 and CCSD(T) complete basis set limit) interaction energies of small model complexes, DNA base pairs, and amino acid pairs. *Phys Chem Chem Phys* 2006, 8:1985.

 © 2011 John Wiley & Sons, Ltd.

17590884, 2011, 3, Downloaded from https://wires.onlinelibrary.wiley.com/doi/10.1002/wcms.40 by TEI of Greece, Wiley Online Library on [11/12/2025]. See the Terms and Conditions (https://onlinelibrary.wiley.com/terms-and-conditions) on Wiley Online Library for rules of use; OA articles are governed by the applicable Creative Commons License

115. Korth M, Lüchow A, Grimme S. Toward the exact solution of the electronic Schrdingier Equation for noncovalent molecular interactions: worldwide distributed quantum Monte Carlo calculations. *J Phys Chem A* 2008, 112:2004.

116. Jurecka P, Hobza P. True stabilization energies for the optimal planar hydrogen-bonded and stacked structures of guanine ... cytosine, adenine ... thymine, and their 9- and 1-methyl derivatives: complete basis set calculations at the MP2 and CCSD(T) levels and comparison with experiment. *J Am Chem Soc* 2003, 125:15608.

117. Sorella S, Casula M, Rocca D. Weak binding between two aromatic rings: feeling the van der Waals attraction by quantum Monte Carlo methods. *J Chem Phys* 2007, 127:014105.

118. Zaccheddu M, Filippi C, Buda F. Anion-pi and pi-pi cooperative interactions regulating the self-assembly of nitrate-triazine-triazine complexes. *J Phys Chem A* 2008, 112:1627.

 © 2011 John Wiley & Sons, Ltd.

17590884, 2011, 3, Downloaded from https://wires.onlinelibrary.wiley.com/doi/10.1002/wcms.40 by TEI of Greece, Wiley Online Library on [11/12/2025]. See the Terms and Conditions (https://onlinelibrary.wiley.com/terms-and-conditions) on Wiley Online Library for rules of use; OA articles are governed by the applicable Creative Commons License